

Lambda Polarization in Polarized Proton-Proton Collisions at RHIC

C. Boros, J.T. Londergan¹ and A.W. Thomas

Department of Physics and Mathematical Physics, and Special Research Center for the Subatomic Structure of Matter, University of Adelaide, Adelaide 5005, Australia

¹ *Department of Physics and Nuclear Theory Center, Indiana University, Bloomington, IN 47408, USA*

(October 24, 2018)

Abstract

We discuss Lambda polarization in semi-inclusive proton-proton collisions, with one of the protons longitudinally polarized. The hyperfine interaction responsible for the Δ - N and Σ - Λ mass splittings gives rise to flavor asymmetric fragmentation functions and to sizable polarized non-strange fragmentation functions. We predict large positive Lambda polarization in polarized proton-proton collisions at large rapidities of the produced Lambda, while other models, based on $SU(3)$ flavor symmetric fragmentation functions, predict zero or negative Lambda polarization. The effect of Σ^0 and Σ^* decays is also discussed. Forthcoming experiments at RHIC will be able to differentiate between these predictions.

I. INTRODUCTION

Measurements of the polarization dependent structure function, g_1 , in deep inelastic scattering [1] have inspired considerable experimental and theoretical effort to understand the spin structure of baryons. While most of these studies concern the spin structure of the nucleons, it has become clear that similar measurements involving other baryons would provide helpful, complementary information [2–9]. The Lambda baryon plays a special role in this respect. It is an ideal testing ground for spin studies since it has a rather simple spin structure in the naive quark parton model. Furthermore, its self-analyzing decay makes polarization measurements experimentally feasible.

Forthcoming experiments at RHIC could measure the polarization of Lambda hyperons produced in proton-proton collisions with one of the protons longitudinally polarized, $p^\uparrow p \rightarrow \Lambda^\uparrow X$. The polarization dependent fragmentation function of quarks and gluons into Lambda hyperons can be extracted from such experiments. These fragmentation functions contain information on how the spin of the polarized quarks and gluons is transferred to the final state Lambda. The advantage of proton proton collisions, as opposed to e^+e^- annihilation, where Λ production and polarization is dominated by strange quark fragmentation, is that Lambdas at large positive rapidity are mainly fragmentation products of up and down valence quarks of the polarized projectile. Thus, the important question, intimately related to our understanding of the spin structure of baryons, of whether polarized up and down quarks can transfer polarization to the Lambda can be tested at RHIC [5].

In a previous publication, we have shown that the hyperfine interaction, responsible for the Δ - N and Σ^0 - Λ mass splittings leads to non-zero polarized non-strange quark fragmentation functions [14]. These non-zero polarized up and down quark fragmentation functions give rise to sizeable *positive* Λ polarization in experiments where the strange quark fragmentation is suppressed. On the other hand, predictions based either on the naive quark model or on $SU(3)$ flavor symmetry predict *zero* or *negative* Lambda polarization [2].

In section II, we briefly discuss fragmentation functions and show how the hyperfine interaction leads to polarized non-strange fragmentation functions. We fix the parameters of the model by fitting the data on Λ production in e^+e^- annihilation. In section III, we discuss Λ production in pp collisions at RHIC energies. We point out that the production of Λ 's at high rapidities is dominated by the fragmentation of valence up and down quarks of the polarized projectile, and is ideally suited to test whether non-strange quarks transfer their polarization to the final state Λ . We predict significant positive Λ -polarization at large rapidities of the produced Λ .

II. FRAGMENTATION FUNCTIONS

Fragmentation functions can be defined as light-cone Fourier transforms of matrix elements of quark operators [12,13]

$$\frac{1}{z} D_{q\Lambda}^\Gamma(z) = \frac{1}{4} \sum_n \int \frac{d\xi^-}{2\pi} e^{-iP^+\xi^-/z} \text{Tr}\{\Gamma \langle 0|\psi(0)|\Lambda(PS); n(p_n)\rangle \langle \Lambda(PS); n(p_n)|\bar{\psi}(\xi^-)|0\rangle\}, \quad (1)$$

where, Γ is the appropriate Dirac matrix; P and p_n refer to the momentum of the produced Λ and of the intermediate system n ; S is the spin of the Lambda and the plus projections

of the momenta are defined by $P^+ \equiv \frac{1}{\sqrt{2}}(P^0 + P^3)$. z is the plus momentum fraction of the quark carried by the produced Λ .

Translating the matrix elements, using the integral representation of the delta function and projecting out the light-cone plus and helicity \pm components we obtain

$$\frac{1}{z}D_{q\Lambda}^\pm(z) = \frac{1}{2\sqrt{2}} \sum_n \delta[(1/z - 1)P^+ - p_n^\pm] |\langle 0 | \psi_\mp^\pm(0) | \Lambda(PS_\parallel); n(p_n) \rangle|^2. \quad (2)$$

Here, $\psi_\mp^\pm = \frac{1}{2}\gamma_- \gamma_+ \frac{1}{2}(1 \pm \gamma_5)\psi$, and we have defined $\gamma_\pm = \frac{1}{\sqrt{2}}(\gamma_0 \pm \gamma_3)$. The fragmentation function of an anti-quark into a Λ is given by Eq. (2), with ψ_+ replaced by ψ_+^\dagger :

$$\frac{1}{z}D_{\bar{q}\Lambda}^\pm(z) = \frac{1}{2\sqrt{2}} \sum_n \delta[(1/z - 1)P^+ - p_n^\pm] |\langle 0 | \psi_+^{\dagger\pm}(0) | \Lambda(PS_\parallel); n(p_n) \rangle|^2. \quad (3)$$

$D_{q\Lambda}^\pm$ can be interpreted as the probability that a quark with positive/negative helicity fragments into a Λ with positive helicity and similarly for antiquarks.

The operator ψ_+ (ψ_+^\dagger) either destroys a quark (an antiquark) or it creates an antiquark (quark) when acting on the Λ on the right hand side in the matrix elements. Thus, whereas, in the case of quark fragmentation, the intermediate state can be either an anti-diquark state, $\bar{q}\bar{q}$, or a four-quark-antiquark state, $qq\bar{q}\bar{q}$, in the case of antiquark fragmentation, only four-antiquark states, $\bar{q}\bar{q}\bar{q}\bar{q}$, are possible assuming that there are no antiquarks in the Λ . (Production of Λ 's through coupling to higher Fock states of the Λ is more complicated and involves higher number of quarks in the intermediate states. As a result it would lead to contributions at lower z values.) Thus, we have

- (1a) $q \rightarrow qq\bar{q} + \bar{q}\bar{q} = \Lambda + \bar{q}\bar{q}$
- (1b) $q \rightarrow qq\bar{q} + qq\bar{q}\bar{q} = \Lambda + qq\bar{q}\bar{q}$,

for the quark fragmentation and

- (2) $\bar{q} \rightarrow qq\bar{q} + \bar{q}\bar{q}\bar{q}\bar{q} = \Lambda + \bar{q}\bar{q}\bar{q}\bar{q}$,

for the antiquark fragmentation.

While, in case (1a), the initial fragmenting quark is contained in the produced Lambda, in case (1b) and (2), the Lambda is mainly produced by quarks created in the fragmentation process. Therefore, we not only expect that Lambdas produced through (1a) usually have larger momenta than those produced through (1b) or (2) but also that Lambdas produced through (1a) are much more sensitive to the flavor spin quantum numbers of the fragmenting quark than those produced through (1b) and (2). In the following we assume that (1b) and (2) lead to approximately the same fragmentation functions. In this case, the difference, $D_{q\Lambda} - D_{\bar{q}\Lambda}$, responsible for leading particle production, is given by the fragmentation functions associated with process (1a).

Similar observations also follow from energy-momentum conservation built in Eqs. (2) and (3). The delta function implies that the function, $D_q(z)/z$, peaks at [14]

$$z_{max} \approx \frac{M}{M + M_n}. \quad (4)$$

Here, M and M_n are the mass of the produced particle and the produced system, n , and we work in the rest frame of the produced particle. We see that the location of the maxima of the fragmentation function depends on the mass of the system n . While the high z region is dominated by the fragmentation of a quark into the final particle and a small mass system, large mass systems contribute to the fragmentation at lower z values. The maxima of the fragmentation functions from process (1a) are given by the mass of the intermediate diquark state and that of the the fragmentation functions from the processes (1b) and (2b) by the masses of intermediate four quark states. Thus, the contribution from process (1a) is harder than those from (1b) and (2).

Energy-momentum conservation also requires that the fragmentation functions are not flavor symmetric. While the assertion of isospin symmetry, $D_{u\Lambda} = D_{d\Lambda}$, is well justified, SU(3) flavor symmetry is broken not only by the strange quark mass but also by the hyperfine interaction. Let us discuss the fragmentation of a u (or d) quark and that of an s quark into a Lambda through process (1a). While the intermediate diquark state is always a scalar in the strange quark fragmentation, it can be either a vector or a scalar diquark in the fragmentation of the non-strange quarks. The masses of the scalar and vector non-strange diquarks follow from the mass difference between the nucleon and the Delta [10], while those of the scalar and vector diquark containing a strange quark can be deduced from the mass difference between Σ and Λ [11]. They are roughly $m_s \approx 650$ MeV and $m_v \approx 850$ MeV for the scalar and vector non-strange diquarks, and $m'_s \approx 890$ MeV and $m'_v \approx 1010$ MeV for scalar and vector diquarks containing strange quarks, respectively [11,14]. According to Eq. (4), these numbers lead to soft up and down quark fragmentation functions and to hard strange quark fragmentation functions.

Energy-momentum conservation, together with the splitting of vector and scalar diquark masses, has the further important consequence that polarized non-strange quarks can transfer polarization to the final state Lambda. To see this we note that the probabilities for the intermediate state to be a scalar or vector diquark state in the fragmentation of an up or down quark with parallel or anti-parallel spin to the spin of the Lambda can be obtained from the $SU(6)$ wave function of the Λ

$$\begin{aligned} \Lambda^\uparrow = & \frac{1}{2\sqrt{3}} [2s^\uparrow(ud)_{0,0} + \sqrt{2}d^\downarrow(us)_{1,1} - d^\uparrow(us)_{1,0} + d^\uparrow(us)_{0,0} + \\ & -\sqrt{2}u^\downarrow(ds)_{1,1} + u^\uparrow(ds)_{1,0} - u^\uparrow(ds)_{0,0}] . \end{aligned} \quad (5)$$

While the u or d quarks with spin anti-parallel to the spin of the Λ are always associated with a vector diquark, u and d quarks with parallel spin have equal probabilities to be accompanied by a vector or scalar diquark. The fragmentation functions of non-strange quarks with spin parallel to the Λ spin are harder than the corresponding fragmentation functions with anti-parallel spins. Thus, $\Delta D_{u\Lambda}$ is positive for large z values and negative for small z . Their total contribution to polarized Lambda production might be zero or very small. Nevertheless, $\Delta D_{u\Lambda}$ and $\Delta D_{d\Lambda}$ can be sizable for large z values, since both $D_{u\Lambda}$ and $\Delta D_{u\Lambda}$ are dominated by the spin-zero component in the large z limit. Furthermore, they will dominate polarized Lambda production whenever the production from strange quarks is suppressed.

The matrix elements can be calculated using model wave functions at the scale relevant to the specific model and the resulting fragmentation functions can be evolved to a higher scale

to compare them to experiments. In a previous paper [14], we calculated the fragmentation functions in the MIT bag model and showed that the resulting fragmentation functions give a very reasonable description of the data in e^+e^- annihilation. Since the mass of the intermediate states containing more than two quarks are not known we only calculate the contributions of the diquark intermediate states in the bag model. The other contributions have been determined by performing a global fit to the e^+e^- data. For this, we used the simple functional form

$$D_{\bar{q}\Lambda}(z) = N_{\bar{q}}z^\alpha(1-z)^\beta \quad (6)$$

to parameterize $D_{\bar{q}\Lambda} = D_{\bar{u}\Lambda} = D_{\bar{d}\Lambda} = \dots D_{\bar{b}\Lambda}$ and also set $D_{g\Lambda} = 0$ at the initial scale, $\mu = 0.25$ GeV.

The fragmentation functions have to be evolved to the scale of the experiment, μ . The evolution of the non-singlet fragmentation functions in LO is given by [15,16]

$$\frac{d}{d\ln\mu^2}[D_{q\Lambda} - D_{\bar{q}\Lambda}](z, \mu^2) = \int_z^1 \frac{dz'}{z'} P_{qq}\left(\frac{z}{z'}\right)[D_{q\Lambda} - D_{\bar{q}\Lambda}](z', \mu^2). \quad (7)$$

The singlet evolution equations are

$$\begin{aligned} \frac{d}{d\ln\mu^2} \sum_q D_{q\Lambda}(z, \mu^2) &= \int_z^1 \frac{dz'}{z'} [P_{qq}\left(\frac{z}{z'}\right) \sum_q D_{q\Lambda}(z, \mu^2) + 2n_f P_{gq}\left(\frac{z}{z'}\right) D_{g\Lambda}(z', \mu^2)] \\ \frac{d}{d\ln\mu^2} D_{g\Lambda}(z, \mu^2) &= \int_z^1 \frac{dz'}{z'} [P_{gq}\left(\frac{z}{z'}\right) \sum_q D_{q\Lambda}(z, \mu^2) + P_{gg}\left(\frac{z}{z'}\right) D_{g\Lambda}(z', \mu^2)], \end{aligned} \quad (8)$$

where the splitting functions are the same as those for the evolution of quark distributions. n_f is the number of flavors. We used the evolution package of Ref. [17] suitably modified for the evolution of fragmentation functions (interchanging the off-diagonal elements in the singlet case).

The results of the LO fit to e^+e^- data [18–23] are shown in Fig. 1. The parameters of our fits are given in Table I. The bag model calculations for $D_{q\Lambda} - D_{\bar{q}\Lambda}$ and $\Delta D_{s\Lambda} - \Delta D_{\bar{s}\Lambda}$ were parametrized using the functional form of Eq. (6). The fragmentation functions, $\Delta D_{u\Lambda} - \Delta D_{\bar{u}\Lambda} = \Delta D_{d\Lambda} - \Delta D_{\bar{d}\Lambda}$, change sign at some value of z , hence we parametrized them using the form

$$\Delta D_{q\Lambda}(z) - \Delta D_{\bar{q}\Lambda}(z) = N_{\bar{q}}z^\alpha(1-z)^\beta(\gamma - z). \quad (9)$$

These parameters are also given in Table I. We also performed a fit using flavor symmetric fragmentation functions which we shall need for the discussion of Lambda production in pp collisions. The fit parameters are given in Table. II. In Fig. 2, we show the calculated fragmentation functions at $Q^2 = M_Z^2$. We note that our fragmentation functions describe the asymmetry in leading and non-leading particle production, as well as the lambda polarization measured in e^+e^- annihilation at the Z pole, very well — as has been shown in Ref. [14].

III. POLARIZED PROTON PROTON COLLISION

Spin-dependent fragmentation of quarks can be studied in proton-proton collisions with one of the protons polarized [5]. Here, many subprocesses may lead to the final state Lambda

so that one has to select certain kinematic regions to suppress the unwanted contributions. In particular, in order to test whether polarized up and down quarks do fragment into polarized Lambdas the rapidity of the produced Lambda has to be large, since at high rapidity, Λ 's are mainly produced through valence up and down quarks. (We count positive rapidity in the direction of the polarized proton beam.)

The difference of the cross sections to produce a Lambda with positive helicity through the scattering of a proton with positive/negative helicity on an unpolarized proton is given in leading order perturbative QCD (LO pQCD) by ¹

$$\begin{aligned}
E_C \frac{\Delta d\sigma}{d^3 p_C}(AB \rightarrow C + X) &= E_C \frac{d\sigma}{d^3 p_C}(A^\uparrow B \rightarrow C^\uparrow + X) - E_C \frac{d\sigma}{d^3 p_C}(A^\downarrow B \rightarrow C^\uparrow + X) \\
&= \sum_{abcd} \int dx_a dx_b dz_c \Delta f_{Aa}(x_a, \mu^2) f_{Bb}(x_b, \mu^2) \Delta D_{cC}(z_c, \mu^2) \\
&\quad \frac{\hat{s}}{\pi z_c^2} \frac{\Delta d\sigma}{d\hat{t}}(ab \rightarrow cd) \delta(\hat{s} + \hat{t} + \hat{u}).
\end{aligned} \tag{10}$$

Here, $\Delta f_{Aa}(x_a, \mu^2)$ and $f_{Bb}(x_b, \mu^2)$ are the polarized and unpolarized distribution functions of partons a and b in protons A and B , respectively, at the scale μ . x_a and x_b are the corresponding momentum fractions carried by partons a and b . $\Delta D_{cC}(z_c, \mu^2)$ is the polarized fragmentation function of parton c into baryon C , in our case $C = \Lambda$. z_c is the momentum fraction of parton c carried by the produced Lambda. $\Delta d\sigma/d\hat{t}$ is the difference of the cross sections at the parton level between the two processes $a^\uparrow + b \rightarrow c^\uparrow + d$ and $a^\downarrow + b \rightarrow c^\uparrow + d$. The unpolarized cross section is given by Eq. (10) with the Δ 's dropped throughout.

The Mandelstam variables at the parton level are given by

$$\hat{s} = x_a x_b s, \quad \hat{t} = -x_a p_\perp \sqrt{s} e^{-y}/z_c, \quad \hat{u} = -x_b p_\perp \sqrt{s} e^y/z_c \tag{11}$$

where, y and p_\perp are the rapidity and transverse momentum of the produced Lambda and \sqrt{s} is the total center of mass energy. The summation in Eq.(10) runs over all possible parton-parton combinations, $qq' \rightarrow qq'$, $qg \rightarrow qg$, $q\bar{q} \rightarrow q\bar{q}$... The elementary unpolarized and polarized cross sections can be found in Refs. [24,25]. Performing the integration in Eq. (10) over z_c one obtains

$$\begin{aligned}
E_C \frac{\Delta d\sigma}{d^3 p_C}(AB \rightarrow C + X) &= \sum_{abcd} \int_{x_{amin}}^1 dx_a \int_{x_{bmin}}^1 dx_b \Delta f_{Aa}(x_a, \mu^2) f_{Bb}(x_b, \mu^2) \Delta D_{cC}(z_c, \mu^2) \\
&\quad \frac{1}{\pi z_c} \frac{\Delta d\sigma}{d\hat{t}}(ab \rightarrow cd)
\end{aligned} \tag{12}$$

with

$$z_c = \frac{x_\perp}{2x_b} e^{-y} + \frac{x_\perp}{2x_a} e^y, \quad x_{bmin} = \frac{x_a x_\perp e^{-y}}{2x_a - x_\perp e^y}, \quad x_{amin} = \frac{x_\perp e^y}{2 - x_\perp e^{-y}} \tag{13}$$

¹Since the relevant spin dependent cross sections on the parton level are only known in LO we perform a LO calculation here.

where $x_{\perp} = 2p_{\perp}/\sqrt{s}$.

In order to elucidate the kinematics, in Fig. 3, we plotted z_c as a function of x_a and y for two different transverse momenta, $p_{\perp} = 10$ GeV (left) and $p_{\perp} = 30$ GeV (right) and for two different values of x_b , $x_b = x_{bmin} + 0.01$ (top) and $x_b = x_{bmin} + 0.1$ (bottom) in Fig. 3. Note, that z_c is maximal both for $x_b = x_{bmin}$ and $x_a = x_{amin}$. With increasing rapidity, y , both the lower integration limit of x_a , x_{amin} , and the momentum fraction of the fragmenting quark transferred to the produced Λ , z_c , increase. Hence, large rapidities probe the fragmentation of mostly valence quarks into fast Lambdas. The dependence on the transverse momenta is also shown in Fig. 3. With increasing p_{\perp} , the kinematic boundary is shifted to smaller rapidities and the fragmentation of the valence quarks can be studied at lower rapidities. This is important since the available phase space is limited by the acceptance of the detectors at RHIC. However, the cross section also decreases with increasing transverse momenta, leading to lower statistics.

In Fig. 4, we show the contributions of the various channels to the cross section for two different transverse momenta, both for inclusive Lambda (4a) and inclusive jet production (4b). $gq \rightarrow gq$ stands, for example, for the contribution to the cross section coming from the subprocess involving a gluon g and a quark q in the initial and final states. In $qq' \rightarrow qq'$, the quarks have different flavors and $q\bar{q}' \rightarrow q\bar{q}'$ is also included. Although the kinematics are not exactly the same for these two processes ² one can study the role played by the fragmentation functions by comparing inclusive Lambda and inclusive jet production. In particular, the contributions from channels containing two gluons in the final state are suppressed in inclusive Lambda production due to the smallness of $D_{g\Lambda}$. We note that $D_{g\Lambda}$ has been set to zero at the initial scale and is generated through evolution. Thus, while $qg \rightarrow qg$ is the dominant channel in inclusive Lambda production, both $qg \rightarrow qg$ and $gg \rightarrow gg$ are equally important in inclusive jet production. There is some ambiguity due to our poor knowledge of the gluon fragmentation — larger probabilities for $g \rightarrow \Lambda$ will enhance the contributions from gluons in inclusive Lambda production. However, the contribution from the process $gg \rightarrow gg$ falls off faster than that from $qg \rightarrow qg$ with increasing rapidity, since $g(x_a)$ decreases faster than $q(x_a)$ with increasing x_a and the Lambdas are produced mainly from valence up and down quarks at high rapidities.

Our analysis of the kinematics and the various contributions to inclusive Lambda production already indicate that Lambda polarization measurements in pp collisions at high rapidities are ideally suited to test whether polarized up and down quarks may fragment into polarized Λ 's. We calculated the Lambda polarization using our flavor asymmetric fragmentation functions for RHIC energies and for $p_{\perp} = 10$ GeV. Increasing the transverse momentum gives similar results, with the only difference that P_{Λ} starts to increase at lower rapidities. We used the standard set of GRSV LO quark distributions for the polarized parton distributions [26] and the LO Cteq4 distributions for the unpolarized quark distributions [27]. The scale, μ , is set equal to p_{\perp} . We also checked that there is only a very weak dependence on the scale by calculating the polarization using $\mu = p_{\perp}/2$ and $\mu = 2p_{\perp}$. The

²While there is only one integration variable, x_a , in inclusive jet production, once p_{\perp} and y are fixed, both x_a and x_b have to be integrated over the allowed kinematic region in inclusive Lambda production, since the produced Λ carries only a fraction of the parton's momentum.

predicted Lambda polarization is shown in Fig 5a. It is positive at large rapidities where the contributions of polarized up and down quarks dominates the production process. At smaller rapidities, where x_a is small, strange quarks also contribute. However, since the ratios of the polarized to the unpolarized parton distributions are small at small x_a the Lambda polarization is suppressed. The result also depends on the parameterization of the polarized quark distributions. In particular, the polarized gluon distribution is not well constrained. However, it is clear from the kinematics that the ambiguity associated with the polarized gluon distributions only effects the results at lower rapidities. This can be seen in Fig. 5b where we plot the contribution from gluons, up plus down quarks and strange quarks to the Lambda polarization.

Next, we contrast our prediction with the predictions of various $SU(3)$ flavor symmetric models which use

$$D_{u\Lambda} = D_{d\Lambda} = D_{s\Lambda}. \quad (14)$$

We fitted the cross sections in e^+e^- annihilation using Eq. (14) and the functional form given in Eq. (6). For the polarized fragmentation functions, we discuss two different scenarios: The model, $SU(3)_A$ (c.f. Fig. 5a), corresponds to the expectations of the naive quark model that only polarized strange quarks can fragment into polarized Lambdas

$$\Delta D_{u\Lambda} = \Delta D_{d\Lambda} = 0 \quad \Delta D_{s\Lambda} = D_{s\Lambda}. \quad (15)$$

It gives essentially zero polarization because the strange quarks contribute at low rapidities where the polarization is suppressed. Model, $SU(3)_B$ (c.f. Fig. 5a), which was proposed in Ref. [2], is based on DIS data, and sets

$$\Delta D_{u\Lambda} = \Delta D_{d\Lambda} = -0.20D_{u\Lambda} \quad \Delta D_{s\Lambda} = 0.60D_{s\Lambda}. \quad (16)$$

This model predicts negative Lambda polarization.

Finally, we address the problem of Lambdas produced through the decay of other hyperons, such as Σ^0 and Σ^* . In order to estimate the contribution of hyperon decays we assume, in the following, that

- (1) the Λ 's produced through hyperon decay inherit the momentum of the parent hyperon
- (2) and that the total probability to produce Λ , Σ^0 or Σ^* from a certain uds state is given by the $SU(6)$ wave function and is independent of the mass of the produced hyperon.

Further, in order to estimate the polarization transfer in the decay process we use the constituent quark model. The polarization can be obtained by noting that the boson emitted in both the $\Sigma^0 \rightarrow \Lambda\gamma$ and the $\Sigma^* \rightarrow \Lambda\pi$ decay changes the angular momentum of the nonstrange diquark from $J = 1$ to $J = 0$, while the polarization of the spectator strange quark is unchanged. Then, the polarization of the Λ is determined by the polarization of the strange quark in the parent hyperon, since the polarization of the Λ is exclusively carried by the strange quark in the naive quark model.

First, let us discuss the case when the parent hyperon is produced by a strange quark. Since the strange quark is always accompanied by a *vector* ud diquark, in both Σ^0 and Σ^* the fragmentation functions of strange quarks into these hyperons are much *softer* than the corresponding fragmentation function into a Λ . Thus, in the high z limit, the contributions from the processes, $s \rightarrow \Sigma^0 \rightarrow \Lambda$ and $s \rightarrow \Sigma^* \rightarrow \Lambda$, are negligible compared to the direct

production, $s \rightarrow \Lambda$. Furthermore, both channels, $s \rightarrow \Sigma^0 \rightarrow \Lambda$ and $s \rightarrow \Sigma^* \rightarrow \Lambda$, enhance the already positive polarization from the direct channel, $s \rightarrow \Lambda$.

This is different in the case when the parent hyperon is produced by an up or down quark. Both Λ and Σ^0 can be produced by an up (down) quark and a *scalar* ds (us) diquark — a process which dominates in the large z limit. (The component with a vector diquark can be neglected in this limit). Furthermore, the up and down fragmentation function of the Σ^* are as important as those of the Λ and Σ^0 in the large z limit. This is because the u fragmentation function of Σ^* peaks at about $1385/(1010 + 1385) \approx 0.58$ which is almost the same as the peak of the *scalar* components of the Λ and Σ , which are $1115/(890 + 1115) \approx 0.57$ and $1190/(890 + 1190) \approx 0.57$, respectively. Thus, for the up and down quark fragmentation, it is important to include the Λ 's from these decay processes.

The relevant probabilities to produce a Λ with positive and negative polarization from a fragmenting up quark with positive polarization and an ds diquark are shown in Table III. We assumed that all spin states of the ds diquark are produced with equal probabilities. The final weights which are relevant in the large z limit are set in bold. We find that if we include all channels, which survive in the large z limit, the polarization of the Λ is reduced by a factor of $10/27$ compared to the case where only the directly produced Λ 's are included. Since the Σ^* decay is a strong decay it is sometimes included in the fragmentation function of the Λ . Including only Σ^* , the suppression factor we obtain is $49/81$. (Note that our model predicts that $u^\uparrow(ds)_{0,0} \rightarrow \Lambda$, $u^\uparrow(ds)_{0,0} \rightarrow \Sigma^0$ and $u^\uparrow(ds)_{1,0} \rightarrow \Sigma^*$ have approximately the same z dependence and are approximately equal (up to the Clebsch-Gordon factors) since the ratios, $M/(M + M_n)$, have roughly the same numerical values. Thus, the effect of the Σ^0 and Σ^* decays can be taken into account by a multiplicative factor.)

In order to illustrate the effect of these decays on the final Λ polarization, we multiplied our results with these factors. The results are shown in Fig. 6b as dotted lines. We note that our implementation of this correction relies on the assumptions that the produced Λ carries all the momentum of the parent hyperon and that all states are produced with equal probabilities. Since neither of these assumptions is strictly valid, we tend to overestimate the importance of hyperon decays. Note also that the inclusion of Σ^0 decay in the $SU(3)$ symmetric models makes the resulting polarization more negative. As a result, even if effects of Σ decays are included, large discrepancies still persist between our predictions and those of $SU(3)$ symmetric models.

IV. CONCLUSIONS

Measurements of the Lambda polarization at RHIC would provide a clear answer to the question of whether polarized up and down quarks can transfer polarization to the final state Λ . We predict *positive* Lambda polarization at high rapidities, in contrast with models based on $SU(3)$ flavor symmetry and DIS which predict *zero* or *negative* Lambda polarization. Our prediction is based on the same physics which led to harder up than down quark distributions in the proton and to the Δ -N and Σ - Λ mass splittings. We also estimated the importance of Σ^0 and Σ^* decays which tend to reduce the predicted Λ polarization.

ACKNOWLEDGMENTS

This work was partly supported by the Australian Research Council. One of the authors [JTL] was supported in part by National Science Foundation research contract PHY-9722706. One author [CB] wishes to thank the Indiana University Nuclear Theory Center for its hospitality during the time part of this work was carried out.

REFERENCES

- [1] EMC Collaboration, J. Ashman et al., Phys. Lett **B206**, 364 (1988).
- [2] M. Burkardt and R.L. Jaffe, Phys. Rev. Lett. **70**, 2537 (1993).
- [3] M. Nzar and P. Hoodbhoy, Phys. Rev. **D 51**, 32 (1995).
- [4] J. Ellis, D. Kharzeev and A. Kotzinian, Z. Phys. **C69**, 467 (1996).
- [5] D. de Florian, M. Stratmann and W. Vogelsang, Phys. Rev. Lett. **81**, 530 (1998).
- [6] C. Boros and A.W. Thomas, Phys. Rev. **D60** (1999) 074017.
- [7] B. Ma, I. Schmidt and J. Yang, Phys. Rev. **D61**, 034017 (2000).
- [8] D. Ashery and H. J. Lipkin, Phys. Lett. **B469**, 263 (1999).
- [9] C. Boros and Liang Zuo-tang, Phys. Rev. **D**, 4491 (1998).
- [10] F. E. Close and A. W. Thomas, Phys. Lett. **B212**, 227 (1988).
- [11] M. Alberg *et al.*, Phys. Lett. **B389**, 367 (1996).
- [12] J. C. Collins and D.E. Soper, Nucl. Phys. **B194**, 445 (1982).
- [13] R. L. Jaffe and X. Ji, Phys. Rev. Lett **71**, 2547 (1993).
- [14] C. Boros, J. T. Londergan and A. W. Thomas, Phys. Rev. **D61**, 014007 (2000).
- [15] J.F. Owens, Phys. Lett. **76B**, 85 (1978).
- [16] T. Uematsu, Phys. Lett. **79B**, 97 (1978).
- [17] M. Miyama and S. Kumano, Comp. Phys. Com. **94**, (1996) 185 and M. Hirai, S. Kumano, and M. Miyama Comp.Phys.Com. **108**, 38 (1998).
- [18] K. Abe et al., SLD Collaboration, Phys. Rev. **D 59**, 052001 (1999).
- [19] D. Buskulic et al., Aleph Collaboration, Z. Phys. **C64**, 361, 1994.
- [20] Abreu et al., Delphi Collaboration, Phys. Lett. **318B**, 249 (1993).
- [21] M. Acciarri et al., L3 Collaboration, Phys. Lett. **B407**, 389 (1997).
- [22] G. Alexander et al., Opal Collaboration, Z. Phys. **C73**, 569 (1997).
- [23] For a compilation of the TASSO, HRS and CELLO data see G. D. Lafferty, P. I. Reeves and M. R. Whalley, J. Phys. G **21**, A1 (1995).
- [24] J. F. Owens, Rev. Mod. Phys. **59**, 465 (1987).
- [25] M. Stratmann and W. Vogelsang, Phys. Lett. **B 295**, 277 (1992).
- [26] M. Gluck et al. Phys. Rev. **D53**, 4775 (1996).
- [27] H.L. Lai et al. Phys. Rev. **D55**, 1280 (1997).

TABLES

TABLE I. Fit parameters obtained by fitting the e^+e^- data. We also parametrized $D_{q\Lambda} - D_{\bar{q}\Lambda}$ and $\Delta D_{q\Lambda} - \Delta D_{\bar{q}\Lambda}$, calculated in the bag.

Parameter	$D_{s\Lambda} - D_{\bar{s}\Lambda}$	$D_{u\Lambda} - D_{\bar{u}\Lambda}$	$D_{\bar{q}\Lambda}$	$\Delta D_{s\Lambda} - \Delta D_{\bar{s}\Lambda}$	$\Delta D_{u\Lambda} - \Delta D_{\bar{u}\Lambda}$
N	5.81×10^9	1.60×10^{17}	99.76	3.73×10^{18}	-6.25×10^{10}
α	21.55	30.49	1.25	21.21	32.48
β	13.60	28.34	11.60	13.38	27.72
γ	—	—	—	—	0.52

TABLE II. Fit parameters obtained by fitting the e^+e^- data and assuming that the fragmentation functions are flavor symmetric.

Parameter	$D_{q\Lambda} - D_{\bar{q}\Lambda}$	$D_{\bar{q}\Lambda}$
N	1.92×10^4	99.76
α	7.47	1.25
β	8.06	11.60

TABLE III. Different channels for the production of Λ hyperons from a positively polarized up quark and a ds diquark. It is assumed that all spin states of the ds diquark are produced with the *same* probabilities. $\Sigma^{*\uparrow}$ and $\Sigma^{*0\uparrow}$ stand for the 1/2 and 3/2 spin component of the Σ^* . See text for further details.

$u(ds)$ states	$u^\uparrow(ds)_{0,0}$			$u^\uparrow(ds)_{1,1}$		$u^\uparrow(ds)_{1,0}$				$u^\uparrow(ds)_{1,-1}$								
relative weights	$\frac{1}{4}$			$\frac{1}{4}$		$\frac{1}{4}$				$\frac{1}{4}$								
products	Λ^\uparrow	$\Sigma^{0\uparrow}$	$\Sigma^{*0\uparrow}$	$\Sigma^{*0\uparrow}$		Λ^\uparrow	$\Sigma^{0\uparrow}$		$\Sigma^{*0\uparrow}$		Λ^\downarrow	$\Sigma^{0\downarrow}$		$\Sigma^{*0\downarrow}$				
relative weights	$\frac{1}{4}$	$\frac{3}{4}$	0	1		$\frac{1}{4}$	$\frac{1}{12}$		$\frac{2}{3}$		$\frac{1}{2}$	$\frac{1}{6}$		$\frac{1}{3}$				
decay products	Λ^\uparrow	Λ^\uparrow	Λ^\downarrow	–	Λ^\uparrow	Λ^\downarrow	Λ^\uparrow	Λ^\downarrow	Λ^\uparrow	Λ^\downarrow	Λ^\uparrow	Λ^\downarrow	Λ^\uparrow	Λ^\downarrow	Λ^\uparrow	Λ^\downarrow		
relative weights	1	$\frac{1}{3}$	$\frac{2}{3}$	0	1	0	1	0	$\frac{1}{3}$	$\frac{2}{3}$	$\frac{2}{3}$	$\frac{1}{3}$	0	1	$\frac{2}{3}$	$\frac{1}{3}$	$\frac{1}{3}$	$\frac{2}{3}$
final weights	$\frac{1}{16}$	$\frac{1}{16}$	$\frac{1}{8}$	0	$\frac{1}{4}$	0	$\frac{1}{16}$	0	$\frac{1}{144}$	$\frac{1}{72}$	$\frac{1}{9}$	$\frac{1}{18}$	0	$\frac{1}{8}$	$\frac{1}{36}$	$\frac{1}{72}$	$\frac{1}{36}$	$\frac{1}{18}$

FIGURES

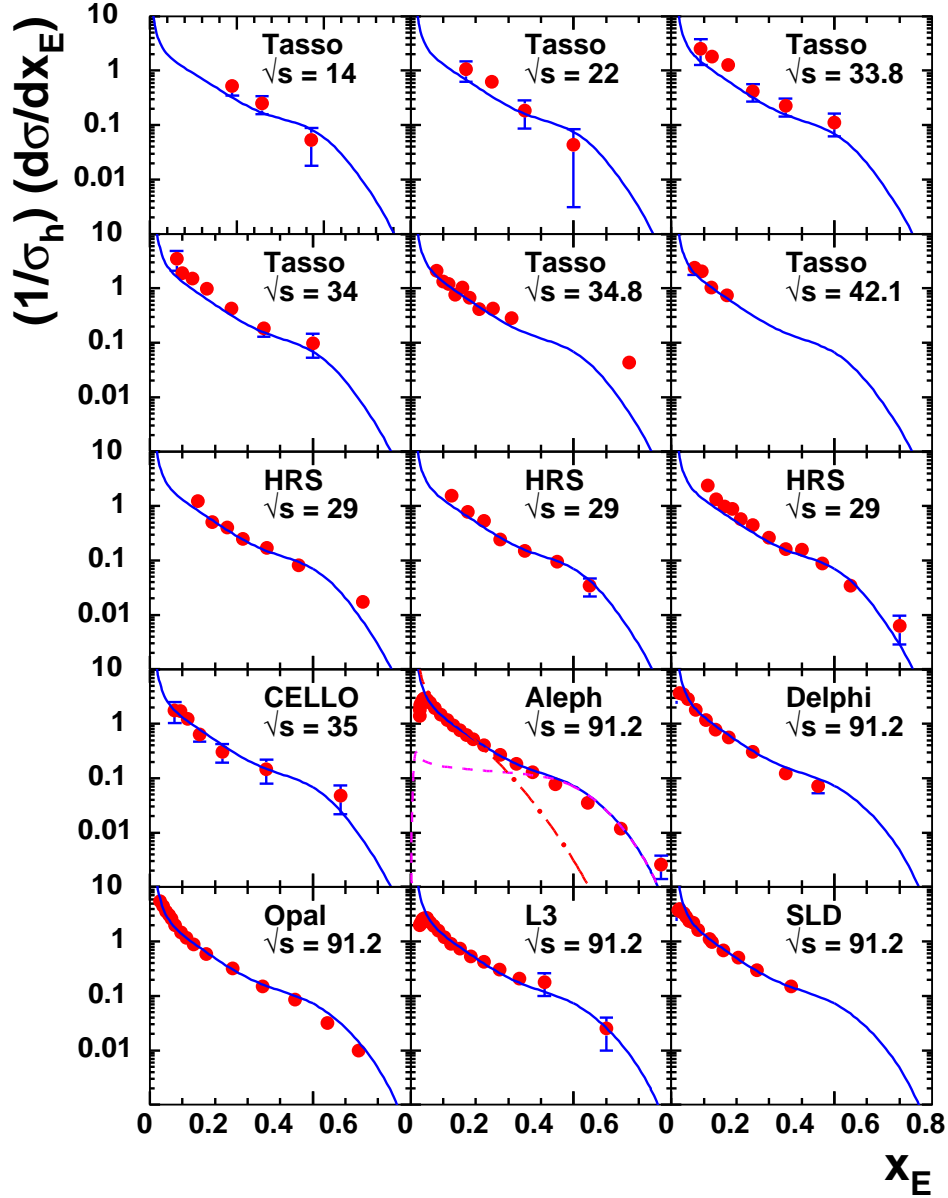


FIG. 1. Inclusive Lambda production in e^+e^- annihilation. The solid lines are the result of the global fit. They contain two parts, the fixed contributions from $D_{q\Lambda} - D_{\bar{q}\Lambda}$ calculated in the bag (dashed line only shown for the Aleph data) and $D_{\bar{q}\Lambda}$ obtained from the fit (dash-dotted line). x_E is defined as $x_E = 2E_\Lambda/\sqrt{s}$ where E_Λ is the energy of the produced Lambda in the e^+e^- center of mass frame and \sqrt{s} is the total center of mass energy.

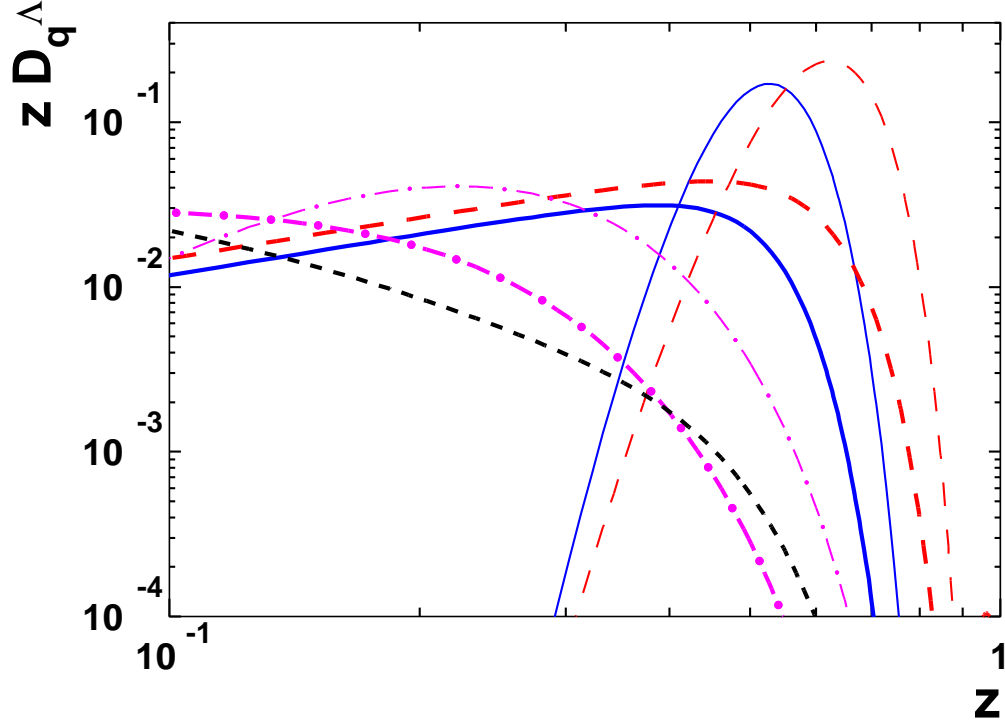


FIG. 2. Fragmentation functions. The solid and dashed lines stand for the calculated fragmentation functions of up and strange quarks into Lambda baryons through production of a Lambda and an anti-diquark and correspond to $D_{u\Lambda} - D_{\bar{u}\Lambda}$ and $D_{s\Lambda} - D_{\bar{s}\Lambda}$, respectively. The dash-dotted line represents the contributions from higher intermediate states, and is obtained by fitting the e^+e^- data and corresponds to $D_{\bar{q}\Lambda}$. The short dashed line is the gluon fragmentation function. The light and heavy lines are the fragmentation functions at the scales $Q^2 = \mu^2$ and $Q^2 = M_Z^2$, respectively. Note that $D_{g\Lambda} = 0$ at $Q^2 = \mu^2$.

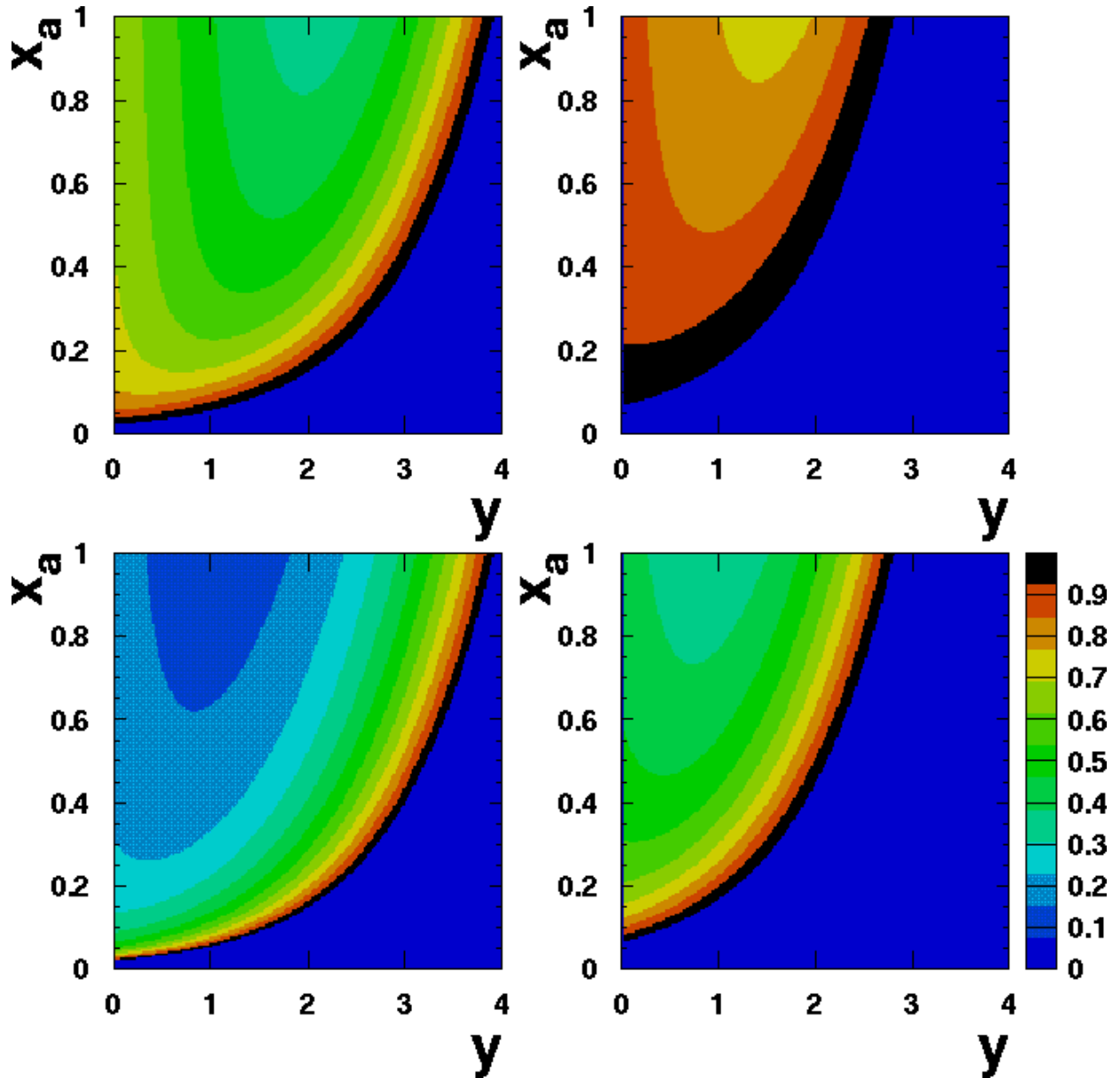


FIG. 3. z_c as a function of x_a and y for two different transverse momenta, $p_\perp = 10$ GeV (left) and $p_\perp = 30$ GeV (right) and for two different values of x_b , $x_b = x_{bmin} + 0.01$ (top) and $x_b = x_{bmin} + 0.1$ (bottom).

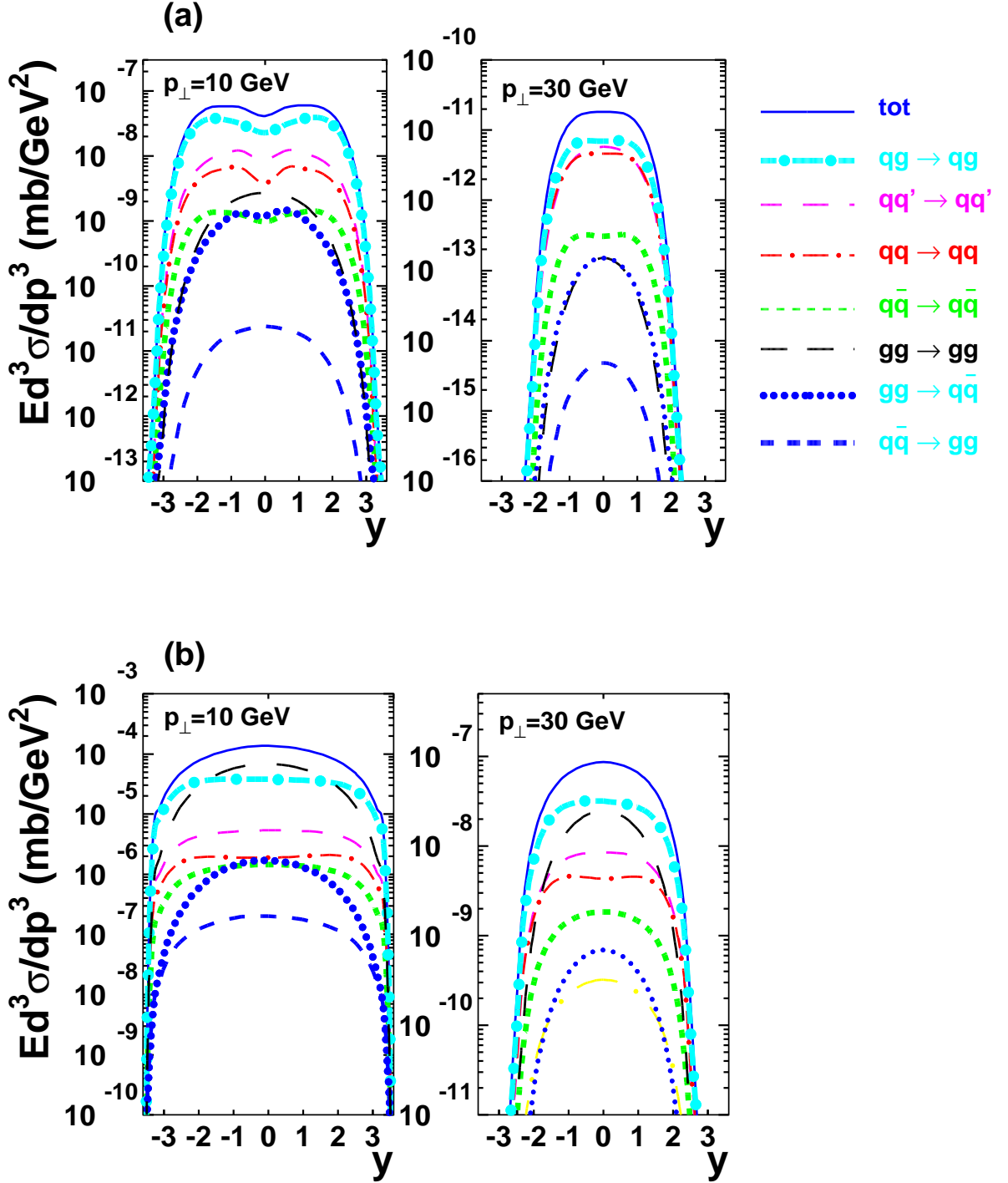


FIG. 4. Contributions from the various channels (a) to the inclusive Lambda production cross section ($pp \rightarrow \Lambda + X$) and (b) to the inclusive jet production cross section ($pp \rightarrow jet + X$) at $p_{\perp} = 10 \text{ GeV}$ (left) and $p_{\perp} = 30 \text{ GeV}$ (right) at $\sqrt{s} = 500 \text{ GeV}$.

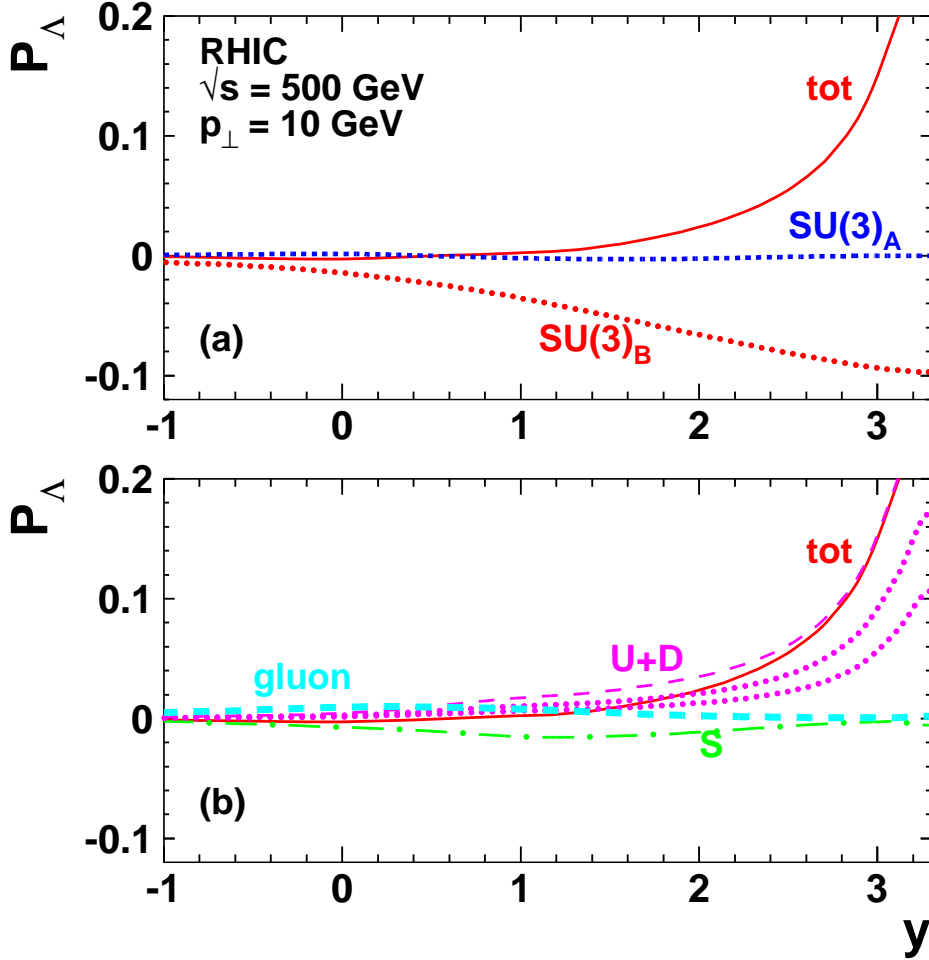


FIG. 5. Lambda polarization at RHIC. (a) The solid line represents our prediction. The predictions of $SU(3)$ symmetric fragmentation models are shown for comparison. The model labeled as $SU(3)_A$ is based on the quark model expectation that only the polarized strange quark may fragment into polarized Lambdas, while $SU(3)_B$, is based on DIS data. (b) Contributions of different flavors to the Λ -polarization. The light dashed, dash-dotted and heavy dashed lines stand for the contributions from up plus down, from strange and from gluon fragmentation, respectively, as calculated here. The estimated polarization including both Σ^0 and Σ^* (lower dotted line) and only Σ^* (upper dotted line) decays are also shown. See text for further details.